

# **Metastability and chimera states in modular delay and pulse-coupled oscillator networks**

Mark Wildie<sup>a)</sup> and Murray Shanahan

*Department of Computing, Imperial College London, 180 Queen's Gate,  
London SW7 2AZ, United Kingdom*

(Dated: 10 October 2012)

Modular networks of delay-coupled and pulse-coupled oscillators are presented that display both transient (metastable) synchronization dynamics and the formation of a large number of “chimera” states characterized by coexistent synchronized and desynchronized subsystems. We consider networks based on both community and small-world topologies. It is shown through simulation that the metastable behavior of the system is dependent in all cases on connection delay, and a critical region is found that maximizes indices of both metastability and the prevalence of chimera states. We show dependence of phase coherence in synchronous oscillation on the level and strength of external connectivity between communities, and demonstrate that synchronization dynamics are dependent on the modular structure of the network. The long-term behaviour of the system is considered and the relevance of the model briefly discussed with emphasis on biological and neurobiological systems.

---

<sup>a)</sup>Electronic mail: mark.wild05@imperial.ac.uk.

Modular systems of identical weakly-coupled oscillators have been shown to exhibit a rich set of dynamics, including metastability and the formation of an unstable procession of concurrently synchronized and desynchronized coalitions, so-called chimera states. The phase-lagged coupling between oscillators employed in previous studies is not an accurate representation of many of the natural systems to which this model can be applied however. Many biological systems are better represented by either delay-coupling, where interaction between oscillators is offset by a fixed time delay, or by a class of pulse-coupled oscillator networks where communication is limited to the exchange of discrete events. It is not obvious that the complex synchronization dynamics found in phase-lagged systems should be present in equivalently structured networks of delay or pulse-coupled oscillators. This paper presents both delay-coupled and pulse-coupled networks that exhibit metastability and chimera states. Unstable synchronization dynamics results from a modular organization consistent with studies of brain connectivity. We show that metastability and the formation and variety of chimera states is dependent on the delay of interaction between oscillators in both cases. Given the potential functional significance of phase-coherence in neuronal communication, we show that increasing connectivity between modular communities is accompanied by phase-coherence between those communities during synchrony.

---

## I. INTRODUCTION

Synchronization is a ubiquitously observed natural phenomenon<sup>1</sup> and the general properties of synchronization within oscillator networks has been the subject of much recent research. Systems of weakly-coupled oscillators have been shown to display a diverse range of behaviors, such as chimera states, formed when a network of identical symmetrically-coupled oscillators spontaneously partitions into synchronized and desynchronized subsets<sup>2-8</sup>, and metastability, characterized by the tendency of a system of oscillators to continuously migrate between a variety of synchronous states<sup>9,10</sup>. The dynamics described by the transient formation of synchronized coalitions of oscillators have been applied to both the function<sup>11,12</sup>

and externally observable phenomena<sup>13</sup> of the brain, and are the prevalent dynamics among many biological, ecological and economic processes.

The Kuramoto model<sup>14</sup> is often used for exploring the synchronization properties of coupled oscillators. Complex chimera-like synchronization behavior, involving the unstable formation of synchronized and desynchronized coalitions of oscillators driven by transitions between metastable states, has been demonstrated in phase-lagged Kuramoto oscillator networks under differing topologies<sup>15,16</sup>. While the continuous exchange of phase information between network participants present in these models is an accurate abstraction of many systems, the detailed operation of the mammalian brain, the all-or-nothing “action potentials” sent over the synapses connecting neurons, is better described by the exchange of a series of discrete events.

Networks of nonlinear pulse-coupled oscillators provide a similarly useful abstraction for studying the synchronization properties of biological systems<sup>17,18</sup>. It is only recently that the transient formation of chimera states found in the dynamics of modularly structured Kuramoto oscillator networks has been examined in detail, and it is not obvious that the same behavior should also be present in pulse-coupled networks of integrate-and-fire relaxation oscillators. If we wish to make the connection between metastable and chimera-like behavior and the potentially functional dynamics of oscillation in neuronal and other pulse-coupled systems, it is necessary to first demonstrate that these networks exhibit a similarly rich repertoire of synchronous behavior.

Moreover, oscillation is prevalent in the aggregate behaviour of neuronal populations<sup>19</sup> and is suggested to play a functionally significant role in the integration and routing of information<sup>20,21</sup>. Networks of weakly-coupled Kuramoto oscillators provide a compelling model of the dynamics of neural systems at this level<sup>22</sup>. Interaction of cortical or sub-cortical structures within the brain is delayed by transmission over the fiber tracts connecting those brain regions however. Propagation velocity and conduction delay varies widely over axonal pathways and species, although conduction velocity can reasonably be estimated to be in the order of 5 – 20 m/s and fast cross-brain axonal conduction delays in the order of 1 – 5 ms in the mammalian brain<sup>23,24</sup>. The dynamics of these systems are more accurately represented by accounting for transmission delay in the network model. Delay-coupled Kuramoto oscillators arranged according to an empirically derived whole brain connectivity matrix have been demonstrated to accurately model resting state fMRI data<sup>13</sup>, but only

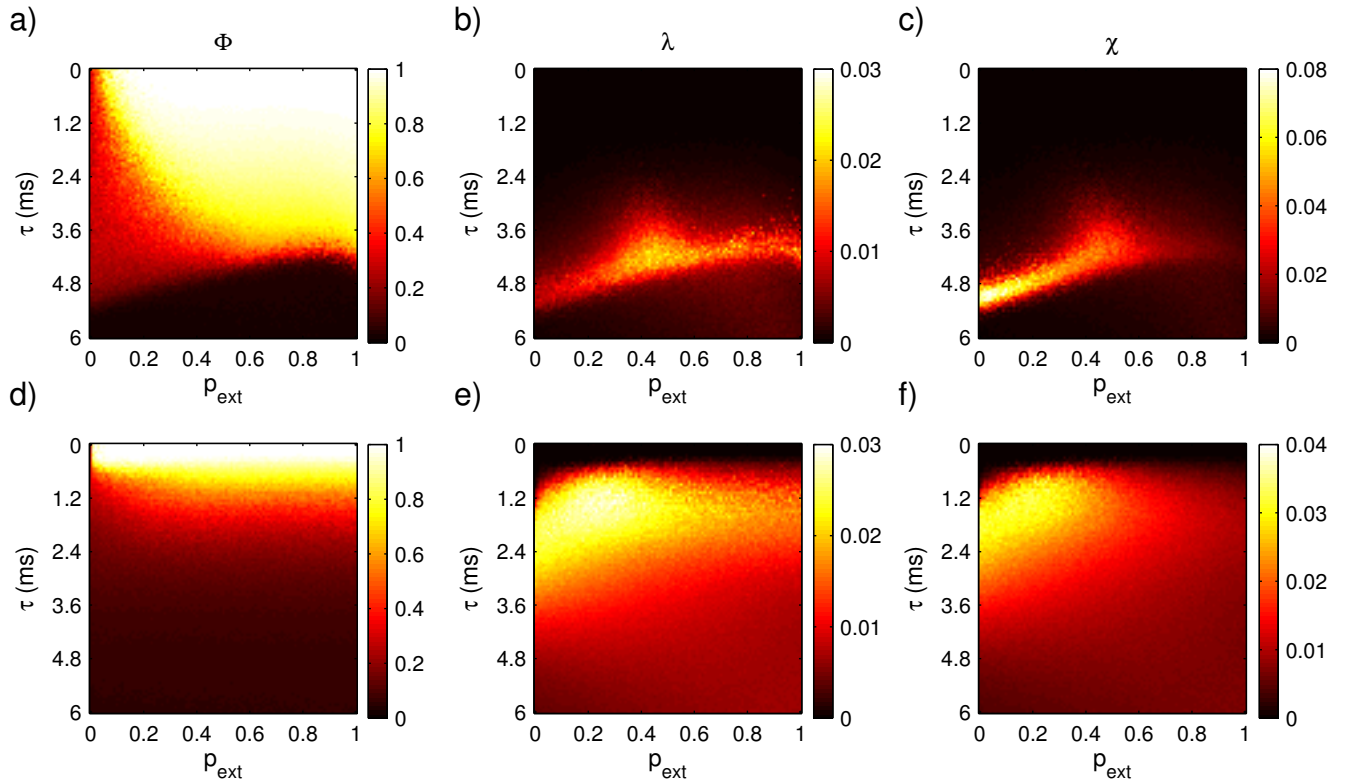


FIG. 1. Global synchrony ( $\Phi$ ) metastability ( $\lambda$ ) and chimera index ( $\chi$ ) for community structured networks of delay-coupled (a,b and c) and pulse-coupled (d,e and f) oscillators. Each data point is the average value over 10 simulations, with parameters divided over a regular  $101 \times 101$  grid. Network connectivity was re-initialized and initial oscillator phases assigned randomly at the start of each simulation. The region of parameter space displaying high values for both indices of metastability and chimera index ( $\lambda$  and  $\chi$ ), indicating complex synchronization dynamics between modular communities within the network, occurs at a transition from global synchrony to disorder associated with increasing delay.

when the dynamics of the network are in a metastable region poised critically between order and disorder.

In the present study we examine the synchronization dynamics of identically structured networks of delay and pulse-coupled oscillators in the presence of modularity and delay. While oscillator networks offer a promising method of elucidating a relationship between connective topology and complex dynamics that appears to be fundamental to the operation of the brain, it remains unclear which properties of empirically derived connectivity matrices are essential to the required dynamics and which are superfluous. We approach

the problem through a systematic investigation of the conditions under which an idealized modular network of oscillators generates metastable chimera states.

We have chosen to use networks of both community<sup>25</sup> and small-world<sup>26</sup> topologies. The human brain has been shown to exhibit modular organization in both underlying structure<sup>27</sup> and activity<sup>28</sup>. The small-world property is commonly found in the biological systems in which we are interested<sup>29,30</sup> and has relevance to the resulting dynamical behavior and synchronization properties<sup>31</sup>. As such, modular networks form a natural basis for exploring competitive behavior within these systems.

This paper is organized as follows. In Section II we introduce the model and describe measures used to characterize the synchronization dynamics of network activity. In Section III we explore the effect of varying connection delay and network modularity, and we demonstrate that delay and phase-lag produce analogous changes in synchronization within a modular network. That is, the transient formation of coalitions of synchronized subsystems within the network accompanied by a transition from global synchrony to disorder. In Section IV we present the main conclusions and summary.

## II. METHODS AND MEASURES

For a network of  $n$  oscillators, the phase  $\theta_i$  of oscillator  $i$  for the Kuramoto model with phase-lagged coupling is governed by the equation

$$\frac{d\theta_i}{dt} = \omega_i + \sum_{j=1}^n K_{i,j} \sin(\theta_j - \theta_i - \alpha) \quad (1)$$

where  $\omega_i$  is the natural frequency of oscillator  $i$ ,  $\alpha$  is a fixed phase-lag, and  $K_{i,j}$  is the connection strength between oscillators  $i$  and  $j$ . For delay-coupling we employ the following modification. The phase of oscillator  $i$  at time  $t + 1$  is governed by

$$\frac{d\theta_i}{dt} = \omega_i + \sum_{j=1}^n K_{i,j} \sin(\theta_j(t - \tau) - \theta_i(t)) \quad (2)$$

where  $\theta_i(t)$  is the phase of oscillator  $i$  at time  $t$  and  $\tau$  is a fixed time delay. For either variant of the model each connection of weight  $K_{i,j} \neq 0$  represents a constant influence exerted by oscillator  $j$  on the phase of oscillator  $i$ .

For the pulse-coupled case we use Mirollo-Strogatz type oscillators<sup>32</sup>. Phase is represented

by the value  $\theta$ , where  $\theta \in [0, 1]$  and advances uniformly at a constant rate in the absence of external input. The state of oscillator  $i$  is given by the smooth, monotonically increasing function

$$f(\theta_i) = y^{-1} \ln [1 + (e^y - 1) \theta_i] \quad (3)$$

where  $f(\theta_i)$  is analogous to the membrane potential used in many neuronal models. The value  $y > 0$  controls the extent to which the function is concave down.

Oscillators in the pulse-coupled case “fire” under the condition  $\theta = 1$  and emit a pulse to all connected oscillators  $j$ , which is received after time delay  $\tau$ . They are reset to phase  $\theta = 0$  after firing. For purely excitatory coupling, the phase of oscillator  $i$  receiving a pulse from a connected oscillator  $j$  is updated according to the rule

$$\theta_i^* = \begin{cases} 1 \rightarrow 0 & \text{for } 1 < f(\theta_i) + \epsilon_{ji} \\ f^{-1}[f(\theta_i) + \epsilon_{ji}] & \text{for } 0 < f(\theta_i) + \epsilon_{ji} < 1 \end{cases} \quad (4)$$

where  $\epsilon_{ji}$  is the weight of the connection from the firing to the receiving oscillator. The delay assigned to each connection represents the time taken for the pulse to travel between the two.

Our network model consists of 256 oscillators partitioned into  $M = 8$  communities of  $N = 32$  oscillators each. Connectivity between oscillators is based on two commonly used modular network topologies. We consider first the community structure described in Ref. 25. Connections were placed between oscillators according to the following rule: for every pair of oscillators  $i$  and  $j$  such that  $i \neq j$ , a directed edge was established from  $j$  to  $i$  with probability  $p_{int}$  if  $i$  and  $j$  belong to the same community (an internal connection) and with probability  $p_{ext}$  if  $i$  and  $j$  belong to different communities (an external connection). To obtain an average of  $c_{int}$  internal connections and  $c_{ext}$  external connections per oscillator we set

$$p_{int} = \frac{c_{int}}{(N - 1)} \quad (5)$$

$$p_{ext} = \frac{c_{ext}}{N(M - 1)} \quad (6)$$

We denote the average number of incoming connections (average in-degree) per oscillator by  $c_n = c_{int} + c_{ext}$ .

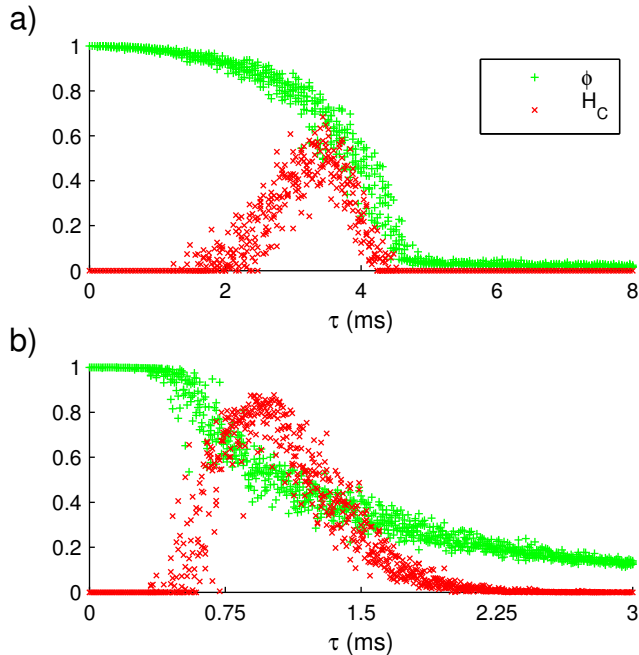


FIG. 2. Global synchrony ( $\Phi$ ) and coalition entropy ( $H_c$ ) for a) delay-coupled and b) pulse-coupled community structured networks. Results are shown for a series of 1000 simulations initialized with a fixed ratio of external connectivity  $p_{ext}$  and increasing delay  $\tau$ .

For every directed edge between oscillators  $i$  and  $j$  there is an associated coupling strength  $k_{i,j}$ , such that  $k_{i,j} = k_{int}$  if  $i$  and  $j$  are connected and belong to the same community, and  $k_{i,j} = k_{ext}$  if  $i$  and  $j$  are connected and belong to different communities. We set  $k_{int}$  and  $k_{ext}$  according to the equations

$$k_{int} = b(a/c_n) \quad (7)$$

$$k_{ext} = (1 - b)(a/c_n) \quad (8)$$

where  $a$  is a constant corresponding to the total input for an average oscillator and  $b$  is a parameter governing the ratio of internal to external input.

We also consider networks with small-world connectivity. Network construction proceeded through a two-phase procedure described in Ref. 33 based on the Watts-Strogatz method<sup>34</sup>. Local connectivity was first established by randomly connecting each oscillator  $i$  to  $s_n$  other oscillators  $j$  within the same community, where  $i \neq j$  and each connection was directed from  $j$  to  $i$ . Inter-community connections were then established by re-wiring, where

for each connection in the network source  $j$  was replaced by a randomly selected oscillator within a different community with probability  $p_r$ . Internal and external connection weights were assigned similarly to community networks, using input and ratio values  $a$  and  $b$  and equations

$$k_{int} = b(a/s_n) \quad (9)$$

$$k_{ext} = (1 - b)(a/s_n) \quad (10)$$

A series of simulations was carried out for each combination of oscillator model and network topology, varying parameters delay  $\tau$ , connection ratio  $b$ , and either  $c_{int}$  and  $c_{ext}$  or  $p_r$  to change the total proportion of internal to external connections between communities. Oscillator phase  $\theta$  was advanced at step size  $1/2\pi$  and equations updated at a resolution  $\omega$  of 0.01 steps. Connectivity was generated independently for each network at the start of simulation and initial oscillator phases assigned randomly. Each simulation was run for 1500 steps with the first 500 discarded to remove any bias on the results from an initial network transient. Statistics were calculated on the remaining 1000 steps.

Generation of connectivity proceeded with parameter value  $c_n = s_n = 8$ , resulting in an average in the community case or total in the small-world case of  $2^{11}$  directed connections per network. Connectivity between oscillators was strictly excitatory with the same weight and delay assigned to each connection within a single network. The total input parameter  $a$  (0.008 for delay-coupled and 0.054 for pulse-coupled networks) was selected from an initial search through the model parameter space and used for all results. For comparison of the results of both models we assume a natural frequency for all oscillators of  $40Hz$ . Pulse-coupled oscillators received parameter value  $y = 5.5$  in all cases.

We quantify the instantaneous synchronization within a single community of oscillators  $c$  at time  $t$  by the measure

$$\phi_c(t) = \left| \left\langle e^{i\theta_k(t)} \right\rangle_{k \in c} \right| \quad (11)$$

where  $\theta_k(t)$  is the phase of oscillator  $k$  at time  $t$  and  $\langle f \rangle_{k \in c}$  denotes the average of  $f$  over all  $k$  in  $c$ . The value ranges from  $[0, 1]$ , with 0 indicating complete desynchronization and 1 complete synchronization. A measure of the global synchrony of the network ( $\Phi$ ) was



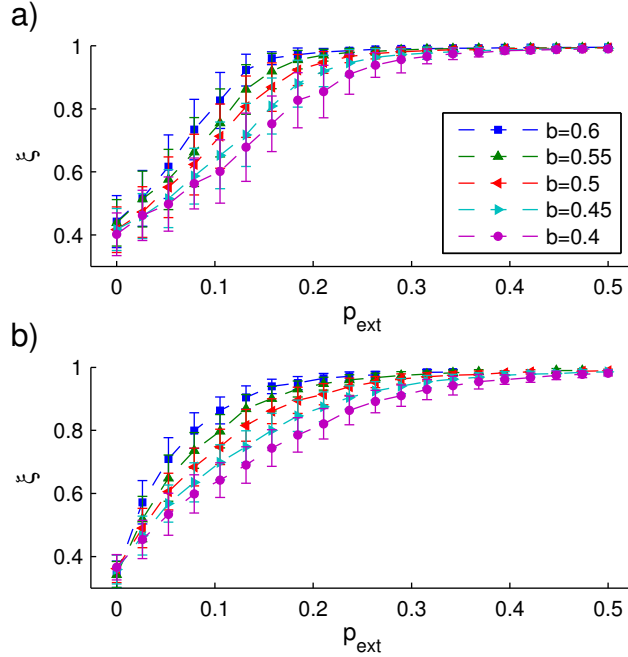


FIG. 3. Average phase coherence between synchronous communities ( $\xi$ ) for a) delay-coupled and b) pulse-coupled community structured networks, with fixed delay and increasing level of external connectivity  $p_{ext}$  and ratio of external connection strength  $b$ . Each data point is the average of 100 simulations.

calculated simply as the average instantaneous synchronization over time of the combined community containing all oscillators in the network.

We define the metastability of the system as the variance in individual community synchrony. Let  $C$  be the set of  $M$  oscillator communities. The variance  $\sigma_c$  of  $\phi_c$  for  $c \in C$  gives an estimate of changes in synchrony for a single community over the simulation period. The average variance  $\langle \phi_c \rangle$  over all communities provides a measure of the metastability (denoted  $\lambda$ ) of the system as a whole. Fixing the time and estimating the variance  $\sigma_{chi}$  across communities gives an instantaneous estimate of how chimera-like the system is, and we use the average variance  $\langle \sigma_{chi} \rangle$  (denoted  $\chi$ ) as an index of this value over time.

Coalition entropy was introduced in Ref. 15 as a measure to describe the variety of metastable states entered by a system of oscillators. The normalized coalition entropy  $H_C$  is given by the equation

$$H_C = \frac{1}{\log_2 |S|} \sum_{s \in S} p(s) \log_2(p(s)) \quad (12)$$

where  $S$  is the set of distinct coalitions the system can generate and  $p(s)$  is the probability of coalition  $s$  arising at any given time. A coalition  $s$  is said to arise at time  $t$  if  $\phi_c(t) > \gamma$  for all  $c \in s$  for some threshold  $\gamma$ , the system of  $M$  communities giving rise to a possible  $2^M$  coalitions. If all coalitions arise with equal probability then  $H_C = 1$ , if the system remains in a single synchronized state then  $H_C = 0$ .

We introduce a similar measure to quantify the phase-coherence of synchronization between communities. We first calculate the instantaneous synchronization  $\phi_c(t)$  and the value

$$\rho_c(t) = \arg \left( \left\langle e^{i\theta_k(t)} \right\rangle_{k \in c} \right) \quad (13)$$

providing both the magnitude ( $\phi_c$ ) and angle ( $\rho_c$ ) of the average synchronization vector across each community  $c$ . For the set of communities  $S$  with magnitude of internal synchronization  $\phi_c > \delta$  for threshold  $\delta$  at time  $t$  we then calculate the value

$$\xi(t) = \left| \left\langle e^{i\rho_k(t)} \right\rangle_{k \in S} \right| \quad (14)$$

We take  $\xi$  as a measure of instantaneous coherence in the phase of oscillation between the set of highly synchronous communities at any time  $t$ .

### III. RESULTS

We first explore changes in the global synchrony and metastability of the system in response to variation in delay and connectivity. A series of  $\sim 10^5$  simulations was carried out for both delay-coupled and pulse-coupled oscillator models arranged in a community structure. Parameters delay  $\tau$  and degree of external connectivity  $p_{ext}$  were varied over the range  $[0, 6]$  ms and  $[0, 1]$  respectively, arranged over a  $101 \times 101$  regular grid with each recorded data point the average over 10 simulations. Parameters  $p_{int}$ ,  $c_{int}$  and  $c_{ext}$  were changed accordingly to maintain average number of connections per oscillator  $c_n = 8$ . The synchrony within each community and global synchrony of the entire system comprising all oscillators was stored at each sub-step of the simulation and used to compute the metastability, chimera index and coalition entropy of the simulation as a whole.

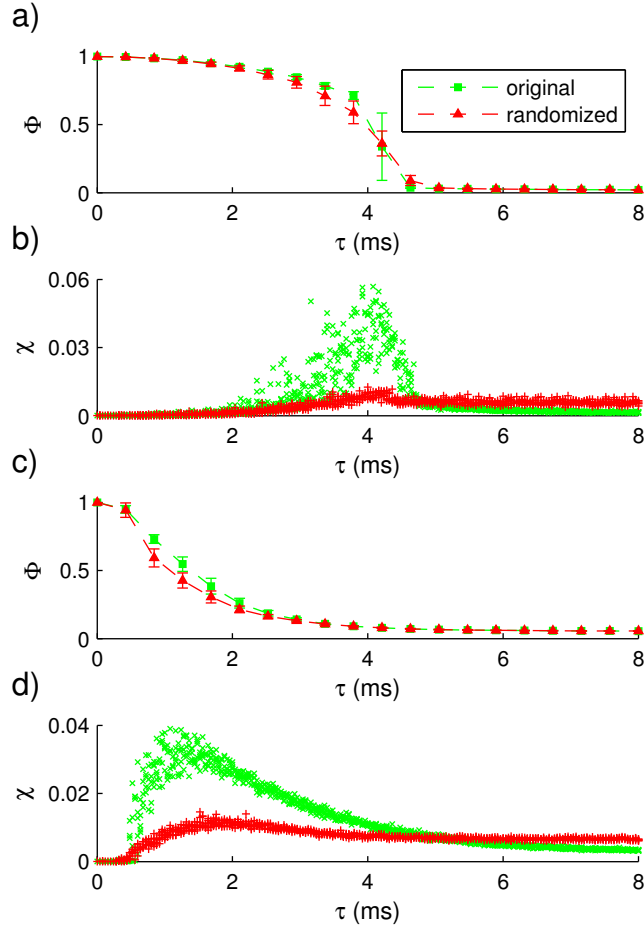


FIG. 4. Comparison of results for community structured networks (green) and randomized versions preserving degree distribution (red). Global synchrony ( $\Phi$ ) is shown for a) delay-coupled and c) pulse-coupled networks for a series of 1000 simulations of varying delay  $\tau$ . Chimera index ( $\chi$ ) is shown for the same b) delay-coupled and d) pulse-coupled networks.

Results are shown in Figure 1. For clarity in the following we use subscripts  $d$  and  $p$  to indicate values corresponding to delay or pulse-coupled networks respectively. In both cases, maximal values for metastability ( $\lambda_d = 0.024$ ,  $\lambda_p = 0.031$ ) and chimera index ( $\chi_d = 0.082$ ,  $\chi_p = 0.037$ ) occur at a point of transition between global synchrony and desynchrony associated with increasing delay. Networks maintain global synchrony when delay is close to zero for external connectivity between communities  $p_{ext}$  up to a small threshold ( $p_{ext} \geq 0.05$  for delay-coupled and  $p_{ext} \geq 0.01$  for pulse-coupled networks). At high values of delay the global synchrony approaches 0 in the delay-coupled case and asymptotically approaches a value of  $\Phi \approx 0.07$  in the pulse-coupled case. Metastability and chimera index are corresponding low

for boundary points  $\Phi$  and reach peak values when global synchrony is in the range  $[0.2, 0.5]$ . Both indices also exhibit a region of optimal modularity as determined by increasing  $p_{ext}$ .

The coalition entropy for a series of 1000 simulations of increasing delay is shown in Figure 2. The ratio of external connectivity  $p_{ext}$  was chosen in each case ( $p_{ext} = 0.5$  for delay-coupled and  $p_{ext} = 0.21$  for pulse-coupled networks) from the optimal region shown in Figure 1. Results exhibit a similar dependence on delay and global synchrony, with maximum coalition entropy  $H_C$  occurring during transition to the desynchronized state. The sensitivity to connection delay is similar to the dependence on phase-lag seen in community structured Kuramoto oscillator networks<sup>15</sup>. A resemblance to thermodynamic phase transition, where fluctuation in synchronization follows from the balance between attracting and repelling forces characterizing ordered and disordered regimes, has been noted previously<sup>14</sup>.

When we consider the effect of connectivity on the behaviour of the system it is interesting to note that results in Figure 1 show high regions for both metastability and chimera index near  $p_{ext} = 0$ , where there are few or no connections between communities. In Figure 3 we show the phase coherence  $\xi$  between the synchronous communities with varying  $p_{ext}$  for fixed delay. Although the networks display metastability for all shown values of  $p_{ext}$ , there is a clear difference in dynamical behaviour as the level of external connectivity is increased. At low values of  $p_{ext}$  variance in synchrony is driven entirely by internal connectivity within each community, and phase coherence between communities remains small. Phase coherence between synchronous communities then increases with external connectivity until complete coherence during synchronization  $\xi = 1$  occurs for values  $p_{ext}$  approximately in the range  $[0.2, 0.5]$  for both delay and pulse-coupled networks. The ratio of internal to external connection strength  $b$  shows a corresponding effect on phase coherence, with increased  $b$  leading to faster convergence on the phase-coherent state.

It is not evident from these results that the metastable synchronization dynamics we observe in modular networks should be stable over time, or should not be present in equivalently structured oscillator networks lacking modularity. We address the effect of modularity on the synchronization dynamics by comparing against results derived using randomized versions of the same networks. Surrogate networks were generated using edge-swapping<sup>35</sup> to preserve degree sequence while randomizing connectivity. Results are shown in Figure 4. Global synchrony displays a transition from high to low values with similar delay profile in both unchanged and randomized networks (Figures 4a and 4c) while values for other indices

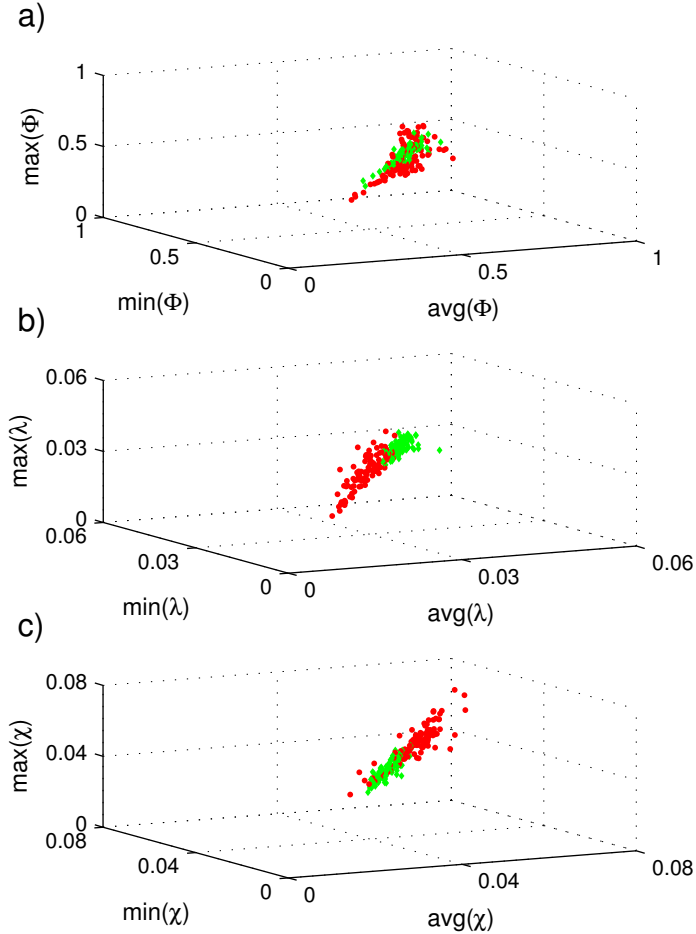


FIG. 5. Long-term behaviour of the system from a series of 100 simulations of  $10^6$  steps each. Minimum, maximum and average values are given for a) global synchrony ( $\Phi$ ) b) metastability ( $\lambda$ ) and c) chimera index ( $\chi$ ) calculated over a 1000 step window. Results for delay-coupled networks are shown in red and pulse-coupled in green.

are significantly reduced (Figures 4b and 4d). We note that, although used in several previous studies, normalization by a random graph of the same degree sequence can produce spurious results if the properties under study scale differently in the randomized version of the network<sup>36</sup>.

Pulse-coupled networks have previously been shown to exhibit long chaotic transients<sup>37,38</sup> resulting in a stable state and an underlying chaotic attractor structure<sup>39,40</sup>. Results for a series of 100 long-term simulations of  $10^6$  steps for the present network are shown in Figure 5. Minimum, maximum and average global synchrony and metastability are given, with values calculated over a 1000 step window. Global synchrony and metastability in all simulations

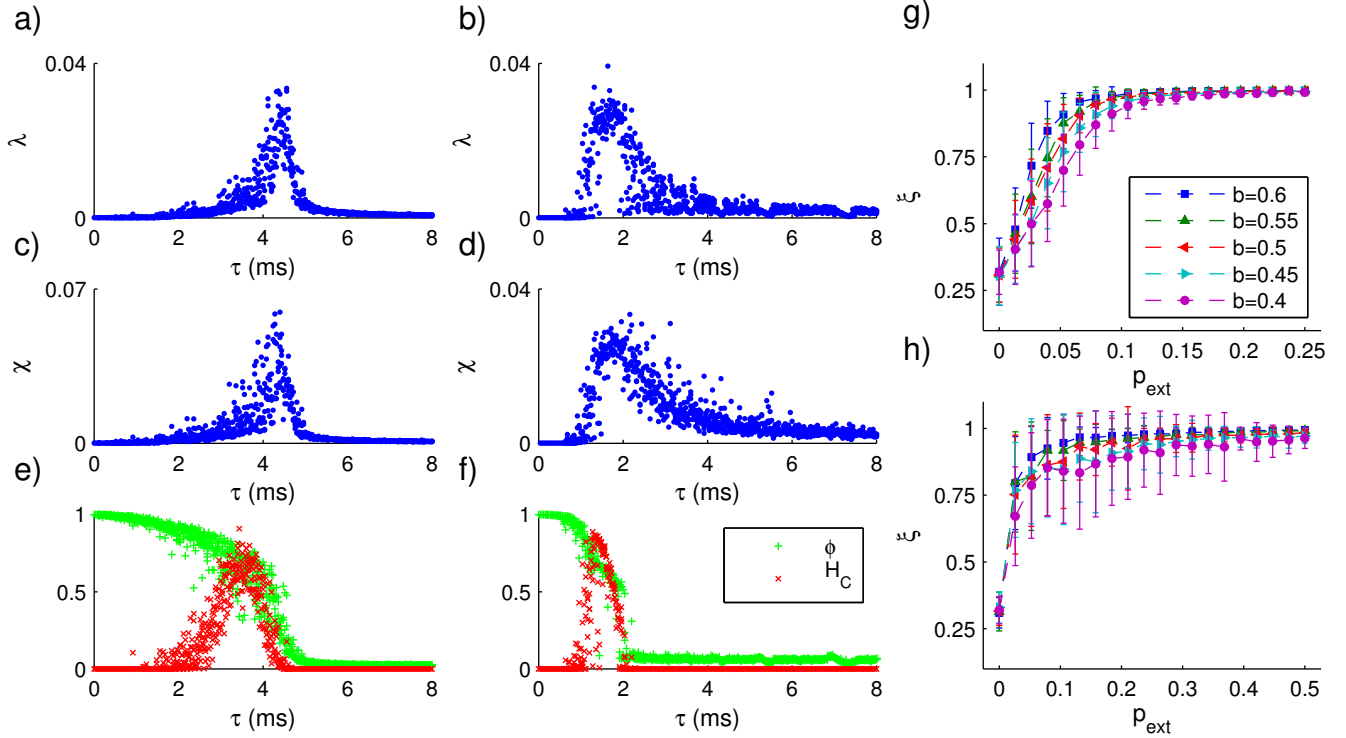


FIG. 6. Results for small-world structured networks. a) Metastability, c) chimera index and e) coalition entropy for 1000 simulations of small-world structured delay-coupled networks for increasing delay and fixed level of external connectivity. b) Metastability, d) chimera index and f) coalition entropy for small-world structured pulse-coupled networks. Phase-coherence  $\xi$  is shown for varying delay  $\tau$  and external connection strength  $b$  for g) delay-coupled and h) pulse-coupled small-world networks.

remained confined to the ranges  $[0.07, 0.72]$  and  $[0.004, 0.053]$  in the delay-coupled case and  $[0.15, 0.73]$  and  $[0.006, 0.049]$  in the pulse-coupled case. None were observed to enter a stable state.

Results repeated using a second modular network topology widely observed in biological systems, the small-world structure, are shown in Figure 6. Network connectivity was initialized in all cases with re-wiring parameter  $p_r = 0.42$ , chosen to maximize indices for both delay and pulse-coupled networks. Although the regions of the parameter space where each index exhibits high values differ between community and small-world networks, both display analogous dynamics. They both exhibit a dependence of global synchrony on delay, with optimal regions for metastability, chimera index and coalition entropy at the transition between the globally synchronous and disordered states (Figures 6a-6f) and a similar

dependence of phase synchrony on external connectivity (Figures 6g and 6h).

#### IV. DISCUSSION

The findings presented in this paper demonstrate the relevance of metastability and chimera-like behavior to the greater understanding of the dynamical properties of delay-coupled and pulse-coupled oscillator networks. Our particular interest lies in theories of neural behavior that posit the importance of episodes of synchronization and desynchronization within given frequency ranges in communication between different areas of the brain. Differences in phase-coherence are suggested to underlie neuronal communication<sup>21,41,42</sup> and oscillators that are both highly synchronous and phase-coherent may represent important functional subgroups within a single synchronous population. The modular structure and small-world properties commonly found in biological networks are duplicated in the current model, although the results are likely applicable to any modular network of delay or pulse-coupled oscillators where chimera-like states may underlie system behavior.

Metastable chimera states are a plausible model of neural dynamics, where they represent the outcome of a competitive process in which a synchronized coalition of oscillators forms while excluding its desynchronized rivals. Phenomena such as binocular rivalry<sup>43</sup> and inattentional blindness<sup>44</sup> attest to the competitive nature of these neuronal processes. Most investigations of chimera-like states to date have focused on the stable condition wherein the chimera state is an attractor, but in neurodynamics a stable chimera state would be pathological. The ever-changing state of the biological brain is better modeled in terms of criticality and metastability<sup>45</sup>. With its underlying dynamics poised between order and disorder, synchronized coalitions of brain processes arise and linger for a while, but then dissolve to be supplanted by new coalitions.

We have shown both delay and pulse-coupled networks to exhibit analogous behaviour to networks of phase-lagged Kuramoto oscillators when delay is treated similarly to the lag parameter in previous studies. Metastability and chimera-states occur in the transition from a fully synchronous to disordered state associated with increasing delay. Additionally we observe a dependence between the degree of modularity of the network and phase coherence between synchronous communities, where a minimum level of external connectivity is required to establish phase-coherent synchrony between communities dependent on con-

nection strength. Unstable synchronization consisting of a series of completely synchronized and desynchronized states has previously been shown in a pulse-coupled network in the presence of noise<sup>39</sup>. In the current model the transition between partially synchronized states results from network structure and delay, the model is absent of stochastic input beyond initialization. That analogous dynamics are replicated over two commonly observed modular network topologies and are significantly reduced by randomization of networks preserving degree sequence supports the validity of the results.

The current model brings the authors closer to a neurologically detailed model exhibiting the high-level formation of coherent oscillating assemblies from the individual activity of spiking neurons, and an understanding of the dynamics generated by the aggregate behaviour of oscillating neuronal populations. It exhibits both the small-world modular organization observed in brain networks<sup>29</sup>, and a range of delay values for generating complex metastable dynamics (within [2.5, 5.5] ms for delay-coupled and [0.5, 3.6] ms for pulse-coupled networks across values  $p_{ext}$ ) that fall within plausible limits of axonal conduction delay<sup>24</sup>. The dependence on modular structure also suggests the optimal ratio of local and long-range connectivity required to produce complex metastable behavior (approximately in the range [0.3, 0.5] in the current model) as a measurable property of neural and other natural delay and pulse-coupled networks.

While tempting to interpret the parameter values of the current model as indicative of synaptic properties required to produce similarly complex neuronal dynamics, demonstration of metastable behavior in biophysical models of large-scale neuronal dynamics<sup>46</sup> will be required to establish correspondence with the biological properties of the mammalian brain. We aim to gain insight into the competitive processes underlying observable brain function through an understanding of the irregular pattern of synchronization present in these networks and corresponding complex dynamical behavior. It remains of great importance to establish a theoretical understanding of the nature of the phenomena described in this and earlier papers.

## REFERENCES

- <sup>1</sup>A. Pikovsky, M. Rosenblum, and J. Kurths, *Synchronization: a universal concept in nonlinear sciences* (Cambridge University Press, 2003).



- <sup>2</sup>D. Abrams and S. Strogatz, Phys. Rev. Lett. **93**, 174102 (2004).
- <sup>3</sup>D. Abrams, R. Mirollo, S. Strogatz, and D. Wiley, Phys. Rev. Lett. **101**, 084103 (2008).
- <sup>4</sup>Y. Kuramoto and D. Battogtokh, Nonlinear Phenom. Complex Syst. **5**, 380–385 (2002).
- <sup>5</sup>E. A. Martens, Phys. Rev. E **82**, 016216 (2010).
- <sup>6</sup>E. A. Martens, Chaos **20**, 043122 (2010).
- <sup>7</sup>O. E. Omel’chenko, Y. L. Maistrenko, and P. A. Tass, Phys. Rev. Lett. **100**, 044105 (2008).
- <sup>8</sup>G. C. Sethia, A. Sen, and F. M. Atay, Phys. Rev. Lett. **100**, 144102 (2008).
- <sup>9</sup>E. Niebur, H. G. Schuster, and D. M. Kammen, Phys. Rev. Lett. **67**, 2753 (1991).
- <sup>10</sup>A. Pluchino and A. Rapisarda, Physica A **365**, 184–189 (2006).
- <sup>11</sup>S. L. Bressler and J. A. Scott Kelso, Trends Cog. Sci. **5**, 26–36 (2001).
- <sup>12</sup>M. G. Kitzbichler, M. L. Smith, S. R. Christensen, and E. Bullmore, PLoS Comput. Biol. **5**, e1000314 (2009).
- <sup>13</sup>J. Cabral, E. Hugues, O. Sporns, and G. Deco, NeuroImage **57**, 130–139 (2011).
- <sup>14</sup>Y. Kuramoto, *Chemical oscillations, waves, and turbulence* (Springer-Verlag, 1984).
- <sup>15</sup>M. Shanahan, Chaos **20**, 013108 (2010).
- <sup>16</sup>J. H. Sheeba, V. K. Chandrasekar, and M. Lakshmanan, Phys. Rev. E **81**, 046203 (2010).
- <sup>17</sup>J. Grasman and M. J. W. Jansen, J. Math. Biol. **7**, 171–197 (1979).
- <sup>18</sup>L. F. Abbott and C. van Vreeswijk, Phys. Rev. E **48**, 1483 (1993).
- <sup>19</sup>G. Buzsáki and A. Draguhn, Science **304**, 1926–1929 (2004).
- <sup>20</sup>F. Varela, J.-P. Lachaux, E. Rodriguez, and J. Martinerie, Nat. Rev. Neurosci. **2**, 229–239 (2001).
- <sup>21</sup>P. Fries, Trends Cog. Sci. **9**, 474–480 (2005).
- <sup>22</sup>M. Breakspear, S. Heitmann, and A. Daffertshofer, Front. Human Neurosci. **4**, 190 (2010).
- <sup>23</sup>A. Ghosh, Y. Rho, A. R. McIntosh, R. Kötter, and V. K. Jirsa, PLoS Comput. Biol. **4**, e1000196 (2008).
- <sup>24</sup>S. S.-H. Wang, J. R. Shultz, M. J. Burish, K. H. Harrison, P. R. Hof, L. C. Towns, M. W. Wagers, and K. D. Wyatt, J. Neurosci. **28**, 4047–4056 (2008).
- <sup>25</sup>M. Girvan and M. E. J Newman, Proc. Natl. Acad. Sci. U.S.A. **99**, 7821–7826 (2002).
- <sup>26</sup>D. J. Watts, *Small worlds: the dynamics of networks between order and randomness* (Princeton University Press, 1999).
- <sup>27</sup>P. Hagmann, L. Cammoun, X. Gigandet, R. Meuli, C. J. Honey, V. J. Wedeen, and O. Sporns, PLoS Biol. **6**, e159 (2008).

- <sup>28</sup>M. Valencia, M. A. Pastor, M. A. Fernández-Seara, J. Artieda, J. Martinerie, and M. Chavez, *Chaos* **19**, 023119 (2009).
- <sup>29</sup>D. S. Bassett and E. Bullmore, *Neuroscientist* **12**, 512–523 (2006).
- <sup>30</sup>O. Sporns and J. D. Zwi, *Neuroinformatics* **2**, 145–162 (2004).
- <sup>31</sup>M. Barahona and L. M. Pecora, *Phys. Rev. E* **89**, 054101 (2002).
- <sup>32</sup>R. E. Mirollo and S. H. Strogatz, *SIAM J. Appl. Math.* **50**, 1645–1662 (1990).
- <sup>33</sup>M. Shanahan, *Phys. Rev. E* **78**, 041924 (2008).
- <sup>34</sup>D. J. Watts and S. H. Strogatz, *Nature* **393**, 440–442 (1998).
- <sup>35</sup>R. Milo., N. Kashtan, S. Itzkovitz, M. E. J. Newman, and U. Alon, arXiv:cond-mat/0312028(2003).
- <sup>36</sup>B. C. M. van Wijk, C. J. Stam, and A. Daffertshofer, *PLoS ONE* **5**, e13701 (2010).
- <sup>37</sup>H. Riecke, A. Roxin, S. Madruga, and S. A. Solla, *Chaos* **17**, 026110 (2007).
- <sup>38</sup>A. Zumdieck, M. Timme, T. Geisel, and F. Wolf, *Phys. Rev. Lett.* **93**, 244103 (2004).
- <sup>39</sup>M. Timme, F. Wolf, and T. Geisel, *Phys. Rev. Lett.* **89**, 154105 (2002).
- <sup>40</sup>P. Ashwin and M. Timme, *Nonlinearity* **18**, 2035–2060 (2005).
- <sup>41</sup>T. Womelsdorf, J. Schoffelen, R. Oostenveld, W. Singer, R. Desimone, A. K. Engel, and P. Fries, *Science* **316**, 1609–1612 (2007).
- <sup>42</sup>S. M. Doesburg, J. J. Green, J. J. McDonald, and L. M. Ward, *PLoS ONE* **4**, e6142 (2009).
- <sup>43</sup>R. Blake, *Brain and Mind* **2**, 5–38 (2001).
- <sup>44</sup>A. Mack, *Curr. Dir. Psychol. Sci.* **12**, 180–184 (2003).
- <sup>45</sup>D. R. Chialvo, *Nature Physics* **6**, 744–750 (2010).
- <sup>46</sup>M. Wildie and M. Shanahan, *Front. Comp. Neurosci.* **5**, 62 (2012).